Available online at www.sciencedirect.com
ScienceDirect
International Journal of Pharmaceutics 350 (2008) 220–229
INTERNATIONAL JOURNAL OF PHARMACEUTICS
www.elsevier.com/locate/ijpharm

Beneficial properties for insulin absorption using superporous hydrogel containing interpenetrating polymer network as oral delivery vehicles

Lichen Yin [a], JieYing Ding [b], Likun Fei [a], Miao He [b], Fuying Cui [b], Cui Tang [a,**], Chunhua Yin [a,b,*]

[a] *State Key Laboratory of Genetic Engineering, School of Life Sciences, Fudan University, Shanghai 200433, China*
[b] *Department of Biochemistry, School of Life Sciences, Fudan University, Shanghai 200433, China*

Received 27 February 2007; received in revised form 27 August 2007; accepted 31 August 2007
Available online 4 September 2007

Abstract

In this investigation, superporous hydrogels containing poly (acrylic acid-*co*-acrylamide)/*O*-carboxymethyl chitosan (*O*-CMC) full-interpenetrating polymer networks (SPH-IPNs) were evaluated for their potentials in effective insulin absorption via the oral route. Insulin release from the SPH-IPNs exhibited sensitivity towards pH and ionic strength. After drug loading and release, the circular dichroism (CD) spectra revealed that conformation of insulin had no significant alteration and bioactivity of insulin was well preserved according to hypoglycaemic effect in mice. Through their abilities to bind Ca^{2+} and to entrap the enzymes, SPH-IPNs could partly inactivate trypsin and α-chymotrypsin, and SPH-IPN with higher *O*-CMC/monomer ratio appeared more potent. Swollen SPH-IPNs could attach mechanically and muco-adhere to the intestinal wall, thus achieving improved retentive properties compared to commonly used muco-adhesive excipient Carbopol® 934. Transport of insulin across rat intestine and colon ex vivo was enhanced around two- to three-fold after application of the SPH-IPN. Insulin-loaded SPH-IPN showed significant hypoglycaemic effects following oral administration to healthy rats, achieving a 4.1% pharmacological availability compared to subcutaneous insulin injection. These pronounced properties demonstrated that the SPH-IPN would be a promising peroral carrier for insulin and other peptide drugs.
© 2007 Published by Elsevier B.V.

Keywords: Insulin; Superporous hydrogels containing full-interpenetrating polymer networks; Enzymatic inhibition; Transport enhancement; Muco-adhesion; Oral administration

1. Introduction

As compared to traditional administration of peptides and proteins such as insulin via subcutaneous injections, oral delivery is a more desirable route because of its lower costs of preparation, good patient compliance and minor side effects (Ziv et al., 1994; Saffran et al., 1997; Aboubakar et al., 2000). However, the bioavailability of insulin through oral administration is very low due to degradation under various proteolytic enzymes in the gastrointestinal (GI) tract and low permeability through the intestinal membrane (Morishita et al., 2004; Aoki et al., 2005). Various strategies have been applied to improving the insulin absorption through intestinal mucosa, including co-administration with absorption enhancers or enzyme inhibitors (Mesiha et al., 1994; Radwant and Aboul-Enein, 2002), chemical modification (Asada et al., 1995) and design of suitable carriers such as nanoparticles (Marschutz et al., 2000) and liposomes (Takeuchi et al., 1996). Nevertheless, these approaches demonstrate low bioavailability and some of them exhibit side effects such as irritation of intestinal mucosal membrane and impairment of the membrane barrier.

During the past few years, peroral delivery systems for peptides and proteins based on superporous hydrogels (SPHs) and SPH composites (SPHCs) have been developed (Dorkoosh et al., 2001, 2002c; Polnok et al., 2004). With the superporous structure, SPHs and SPHCs swell quickly and absorb large amount of

* Corresponding author at: State Key Laboratory of Genetic Engineering, School of Life Sciences, Fudan University, Shanghai 200433, China. Tel.: +86 21 6564 3797; fax: +86 21 5552 2771.
** Corresponding author. Tel.: +86 21 6564 3556; fax: +86 21 5552 2771.
E-mail addresses: tangcui@fudan.edu.cn (C. Tang), chyin@fudan.edu.cn (C. Yin).

0378-5173/$ – see front matter © 2007 Published by Elsevier B.V.
doi:10.1016/j.ijpharm.2007.08.051

water when delivered into the intestine, resulting in mechanical attachment to the gut wall and opening of the tight junctions by mechanical pressure (Dorkoosh et al., 2002a,b). They can also partly inhibit the activity of trypsin, based on their abilities of Ca^{2+} binding and enzyme entrapment (Dorkoosh et al., 2001). Nevertheless, due to extremely small fraction of the polymer in the swollen state, SPHs and SPHCs have weak mechanical properties and thus are easily broken into pieces upon application of stresses, which would result in the decrease of their capacities of enzyme inhibition and mechanical attachment.

In our previous investigation, superporous hydrogels containing poly(acrylic acid-*co*-acrylamide)/*O*-carboxymethyl chitosan interpenetrating polymer networks (SPH-IPNs) were synthesized as a potential peroral delivery system for peptides and proteins (Yin et al., 2007). After introduction of the full-IPN structure, mechanical properties including compressive and tensile moduli of the polymer were significantly improved without loss of its porosity and fast swelling. Existence of *O*-carboxymethyl chitosan (*O*-CMC) also contributed to the enhanced in vitro muco-adhesive force of the SPH-IPNs. In current investigation, the SPH-IPNs were further evaluated for their potentials in effective peroral delivery for peptides and proteins. Using insulin as a model drug, the drug release from the SPH-IPNs was investigated in response to pH and ionic strength. Conformational change and bioactivity stability of insulin following drug loading and release were studied using circular dichroism (CD) spectroscopy and hypoglycaemic effect in mice, respectively. The capabilities of the SPH-IPNs for trypsin and α-chymotrypsin inactivation, Ca^{2+} and Zn^{2+} binding, transport enhancement of insulin across rat intestine and colon, mechanical attachment, and in situ muco-adhesion were also investigated. Finally, intestinal absorption of insulin in rats was investigated following oral administration of insulin-loaded SPH-IPNs.

2. Materials and methods

2.1. Materials

SPH-IPNs were synthesized in our laboratory as described previously (Yin et al., 2007), and samples with *O*-CMC/monomer ratios (w/w) of 0.048, 0.096, 0.144 and 0.192 were designated to be SPH-IPN_{48}, SPH-IPN_{96}, SPH-IPN_{144} and SPH-IPN_{192}, respectively. Trifluoroacetic acid (TFA) and 2-(*N*-morpholino)ethane-sulfonic acid (MES) were purchased from Sigma (St. Louis, MO, USA). Titriplex® III (ethylene dinitrilotetraacetic acid, dinatrium salt) was from Merck (Darmstadt, Germany). Monocomponent insulin crystals (28 IU/mg, from porcine pancreas) were purchased from Xuzhou Biochemical Co. (Xuzhou, China). Trypsin and α-chymotrypsin (from bovine pancreas, 1000 u/mg and 4000 ATEE u/mg, respectively) were purchased from Shanghai Bo'ao Biotechnique Co. Ltd. (Shanghai, China). Enteric-coated capsules for rats were obtained from Chaozhou Pharmaceutical Capsule Factory (Chaozhou, China). Acetonitrile (Merck, Germany) was of HPLC grade. Water used was double distilled. All other chemicals and reagents used were of analytical grade.

Male Sprague–Dawley rats weighing 200–250 g were purchased from the Animal Centre of Fudan University (China), and raised in a room with constant temperature, relative humidity and a standard light/dark cycle. Animal experiments were performed according to the Guiding Principles for the Care and Use of Experiment Animals in Fudan University.

2.2. In vitro release

Insulin loading was performed at 37 °C by immersing 40 mg of the SPH-IPN_{144} in 4 ml 1.5 mg/ml of insulin solution as described previously (Yin et al., 2007), which was subsequently vacuum-dried to constant weight at ambient temperature. In vitro release profiles of the insulin-loaded SPH-IPN_{144} were studied in response to pH and ionic strength. For pH-responsive release, HCl solution (pH 1.0), citrate phosphate buffer (pH 3.0–6.2) and phosphate buffered saline (PBS, pH 7.4) were used as release media. To examine the effect of ionic strength, PBS (ionic strength of 1 and 0.1 M, pH 7.4) and NaCl solutions (ionic strength of 0.01 and 0.001 M, pH 7.0) were used. The dried insulin-loaded SPH-IPNs were immersed into a glass bottle filled with 25 ml of release medium at 37 ± 1 °C. The bottle was shaken at 150 rpm. At predetermined time intervals, 150 μl of the sample was withdrawn and another 150 μl of release medium was added to maintain a constant volume. Samples were centrifuged at 12,000 rpm for 5 min before analysis by HPLC as described previously (Yin et al., 2007).

2.3. Insulin stability

2.3.1. Conformational stability

The release solution (0.01 M PBS, pH 7.4) as mentioned in Section 2.2 was collected and insulin concentration was adjusted to 150 μg/ml. As a control, 0.01 M PBS (pH 7.4) containing 150 μg/ml of insulin was prepared. The conformational characteristics of insulin were examined by CD on a Jasco-715 CD spectrophotometer (Tokyo, Japan). Five scans were performed and averaged for each sample and CD spectrum was obtained by subtracting the PBS spectrum from the preliminary spectrum with noise reduction.

2.3.2. Bioactivity stability

Insulin solution in 0.01 M PBS (pH 7.4) served as a control. The control solution and insulin release solution (0.01 M PBS, pH 7.4) were subcutaneously injected to normal mice at a dose of 0.5 IU/kg, respectively. Blood samples were collected before dosing and 40 min after dosing. After blood sampling, the serum was separated by centrifugation at 12,000 rpm for 4 min. Serum glucose levels were determined using a Glucose GOD-PAD kit (Shanghai Kexin Biochemical Reagent Industry, Shanghai, China). Post-dose blood glucose levels were expressed as the percentage of pre-dose blood glucose levels.

2.4. Enzymatic inhibition

SPH-IPNs were investigated for their potentials in inactivating trypsin and α-chymotrypsin, which are the two most

predominant proteolytic enzymes in the intestinal tract. The enzymatic inhibition of the SPH-IPNs was studied as described previously (Dorkoosh et al., 2001). Briefly, 40 mg of the SPH-IPNs were allowed to swell in 10 ml of trypsin or α-chymotrypsin solution (dissolved in Tris buffer containing 1 mM $CaCl_2$, pH 7.4) at 37 °C. After 30 min, 10 ml of 100 μg/ml insulin solution was added. As a positive control, no polymer was added while as a negative control, only insulin solution was kept under the same condition. All incubations were performed at 37 °C. At timed intervals, 100 μl of samples were taken and diluted with 150 μl of TFA solution (pH 1.8) to stop the enzyme activity. The degradation of insulin was studied by determining the residual amount of insulin using HPLC.

2.5. Ca^{2+} and Zn^{2+} binding

The capability of SPH-IPNs for Ca^{2+} and Zn^{2+} binding was investigated according to the reported method (Dorkoosh et al., 2001) with some modifications. For Ca^{2+} binding, 30 mg of the SPH-IPNs was placed in 4 ml of 40 μg/ml $CaCl_2$ solution in MES/KOH buffer (pH 7.2, containing 250 mM mannitol) for 24 h. The residual solution was measured for free calcium by complexometric titration with Titriplex® III, using calcein as an indicator. The SPH-IPNs were then washed six times with MES/KOH buffer to take out the previously entrapped calcium (unbound Ca^{2+}), which was also measured by complexometric titration. The bound calcium was thereby calculated by subtracting the amount of both free and entrapped calcium from the total amount of calcium in each $CaCl_2$ solution. As for Zn^{2+}, other procedures were the same except that 200 μg/ml $ZnCl_2$ solution was used and the Zn^{2+} content was analyzed by a Zeeman Z-5000 atomic absorbance spectrometer (Hitachi, Japan).

2.6. Mechanical fixation

The mechanical attachment of SPH-IPNs in rat intestine was investigated according to the reported method (Dorkoosh et al., 2002a) with some modifications. Male rat was sacrificed and its jejunum was isolated. A 12-cm jejunum piece was put in a glass tube with length of 10 cm and inner diameter of 6 mm, and 20 mg of $SPH\text{-}IPN_{48}$ or $SPH\text{-}IPN_{192}$ was placed into one end of the jejunum. The whole system was then immersed in 0.01 M PBS (pH 7.4) where the polymer could swell completely. Both ends of the jejunum were tied up to the tube and a horizontal force was introduced when the whole system was centrifuged horizontally at 500 rpm for 5 min. The lateral movement of the polymer along the intestine was considered to show its capability to mechanically attach to the gut wall. As a positive control, 1 ml of 0.5% (w/v) Carbopol® 934P gel was used, which exhibited high muco-adhesive characteristics. The amount of horizontal force (F) which was applied to the polymer could be calculated from the following equation:

$$F = \frac{m \times V^2}{r}$$

where m is the weight of the polymer (kg), r is the radius of centrifuge plate (m) and V is the velocity.

2.7. In situ muco-adhesion

The SPH-IPNs were ground into powders with diameters of 150–200 μm prior to use. Male rats were anesthetized by an intraperitoneal injection of 40 mg/kg body weight of sodium pentobarbital and placed on a heating pad to maintain a body temperature of 37 ± 1 °C. Following a midline incision in the abdomen, a 10-cm jejunum or ileum segment was isolated and carefully washed with pre-warmed PBS to remove intestinal content. Thirty milligrams of the polymer powders were administered to each loop with 2 ml PBS and remained left in the segments for 1 h. As a positive control, 30 mg of Carbopol® 934P was administered with water. The loops were thereafter washed with water at 1.0 ml/s for 1 min using a peristaltic pump. The detached polymers were collected, vacuum-dried and weighed. The muco-adhesive capacity (%) was calculated as the following equation:

$$\text{The muco-adhesive capacity (\%)} = \frac{(\text{the initial amount} - \text{the collected amount}) \times 100}{\text{the initial amount}}.$$

2.8. Transport of insulin across rat intestine and colon

Freshly isolated rat duodenum, jejunum, ileum and colon were washed with Kreb's-Ringer buffer and cut into pieces of about 4 cm each with one end tied up with a silk thread. Ten milligrams of $SPH\text{-}IPN_{144}$ loaded with 0.5 mg insulin were placed into the piece of tissue, followed by adding of 0.5 ml of Kreb's-Ringer buffer and tying up the other open end with a silk thread to form a sac. As a negative control, 0.5 ml of insulin solution (1 mg/ml) was placed in the sac. The filled sacs were immersed in the container filled with 6 ml of oxygenated Kreb's-Ringer buffer, which was shaken smoothly at 37 ± 1 °C. Two hundred microliters of samples were withdrawn from the serosal side at timed intervals and analyzed by HPLC.

2.9. In vivo absorption study

2.9.1. Oral administration

Male rats were fasted for 16 h prior to experiment, but given water ad libitum. Drug administration and blood sampling were conducted without anesthesia. Considering the fact that about 25% of the insulin was released under the pH condition of the stomach, drug-loaded SPH-IPNs were loaded in enteric-coated capsules for rats (3 mm in length and 1.5 mm in diameter). The capsules were made from gelatin and enterosoluble acrylic resin according to Chinese Pharmacopoeia (2000), so that they would not be dissolved until they reached the upper small intestine and thus resulting in drug release in the intestine. Following formulations were applied to the rats: (1) subcutaneous injection of insulin (1 IU/kg); (2) oral administration of enteric-coated capsules for rats (3 mm in length and 1.5 mm in diameter) containing insulin-loaded $SPH\text{-}IPN_{144}$ (40 IU/kg); (3) oral administration of enteric-coated capsules for rats containing blank $SPH\text{-}IPN_{144}$ as a negative control; (4) oral administration of insulin solu-

tion (40 IU/kg). Blood samples were collected from the tail vein immediately before dosing and 0.25, 0.5, 1, 2, 3, 4, 5, 6, 7, 8, 10 and 12 h after dosing. The plasma was centrifuged at 12,000 rpm for 4 min and blood glucose levels were determined using a Glucose GOD-PAD kit.

2.9.2. Pharmacological availability

Post-dose blood glucose levels were expressed as a percentage of pre-dose blood levels. The extent of hypoglycaemic was calculated as the area above the blood glucose level–time curve ($[AAC]_{p.o.}$ and $[AAC]_{s.c.}$) for 0–8 h. The relative pharmacological availability (PA(%)) of the orally administered insulin could be calculated from the following equation:

$$PA(\%) = \frac{([AAC]_{p.o}/dose_{p.o.}) \times 100}{([AAC]_{s.c.}/dose_{s.c.})}$$

Statistical analysis was performed using the analysis of variance method. Differences between group means were judged to be significant at $p < 0.05$.

3. Results and discussion

3.1. In vitro release

3.1.1. Effect of pH on insulin release

As shown in Fig. 1, insulin release from SPH-IPN_{144} exhibited sensitivity towards pH. When pH increased from 1.0 to 6.2, the release rate increased and more insulin was released at the end of the experiment (2 h). At pH 6.2 and 7.4, the release behavior appeared similar in that more than 80% of the insulin was released within 30 min and the remaining insulin was almost released up within 2 h. At pH 1.0 and 3.0, carboxylic groups of the polymeric chains were protonated, leading to shrinkage of the hydrogel and formation of hydrogen bonding between insulin and the polymer. Therefore, insulin release was restricted. When pH reached 4.9, the carboxylic groups on the polymeric chains were partly ionized and significant swelling of the hydrogel occurred, thus facilitating insulin release from the SPH-IPNs. However, only 70% of the insulin was released after 2 h, which might be attributed to the electrostatic interaction between positively charged insulin (p*K*a of insulin being 5.4) and the negatively charged SPH-IPNs. At pH 6.2 and 7.4, the carboxylic groups were completely ionized and the SPH-IPNs were fully swollen. The high swelling ratios of SPH-IPNs and the electrostatic repulsion between the negatively charged insulin and the hydrogel resulted in the rapid and complete release of insulin.

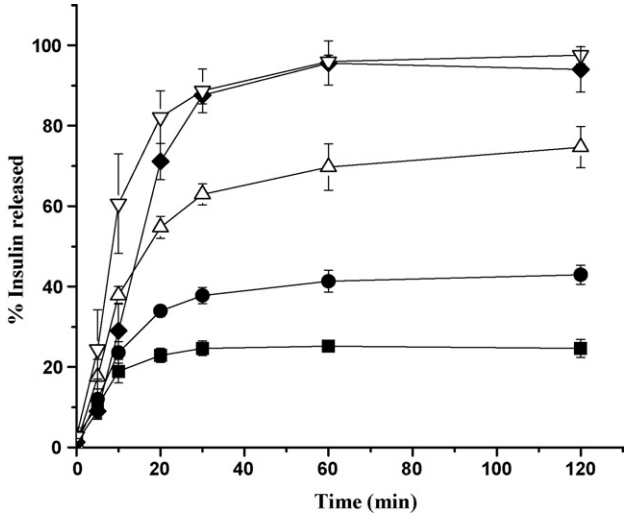

Fig. 1. Cumulative release profiles of insulin from SPH-IPN_{144} at pH: (■) 1.0 (HCl solution); (●) 3.0 (citrate phosphate buffer); (△) 4.9 (citrate phosphate buffer); (♦) 6.2 (citrate phosphate buffer), and (▽) 7.4 (phosphate buffer), respectively. Data were expressed as mean ± S.D. of three experiments.

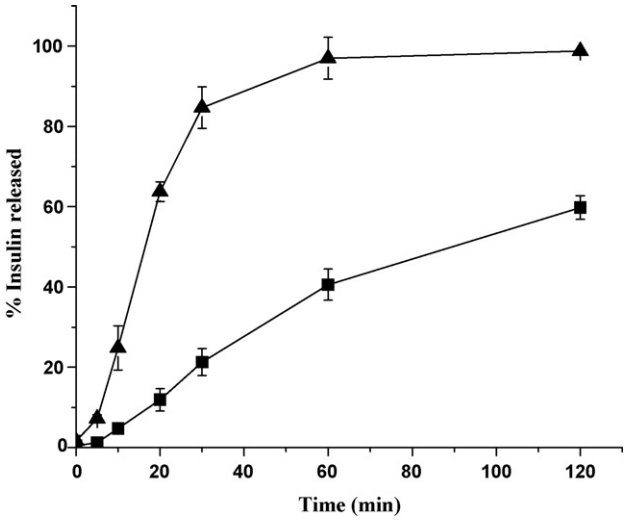

Fig. 2. Effect of ionic strength on cumulative release profiles of insulin from SPH-IPN_{144} (pH 7.0): (■) 1 M; (▲) 0.1 M. Cumulative released insulin under 0.01 and 0.001 M was too little to be detected by HPLC. Data were expressed as mean ± S.D. of three experiments.

3.1.2. Effect of ionic strength on insulin release

Fig. 2 shows the release profiles of insulin under different ionic strength. About 60 and 99% of the insulin was released within 2 h under the ionic strength of 1 and 0.1 M, respectively. Almost no insulin was released when the ionic strength was lower than 0.01 M. Under ionic strength of 1 M, the SPH-IPN slightly swelled due to the strong "charge screening effect", so that release of insulin was retarded and incomplete. Under ionic strength of 0.1 M, the SPH-IPN swelled, leading to the rapid release of insulin. However, more insulin was released within 2 h when compared to release under pH 1.0, which might be due to the electrostatic repulsion between negatively charged insulin and the polymer in the alkaline release medium. When the ionic strength was still lowered, insulin was not dissolved and thus could not be released.

3.2. Stability

3.2.1. Conformational stability

Conformational change and aggregation of peptides have been important subjects to be solved when considering formulations. Currently, physical stability of insulin during drug loading

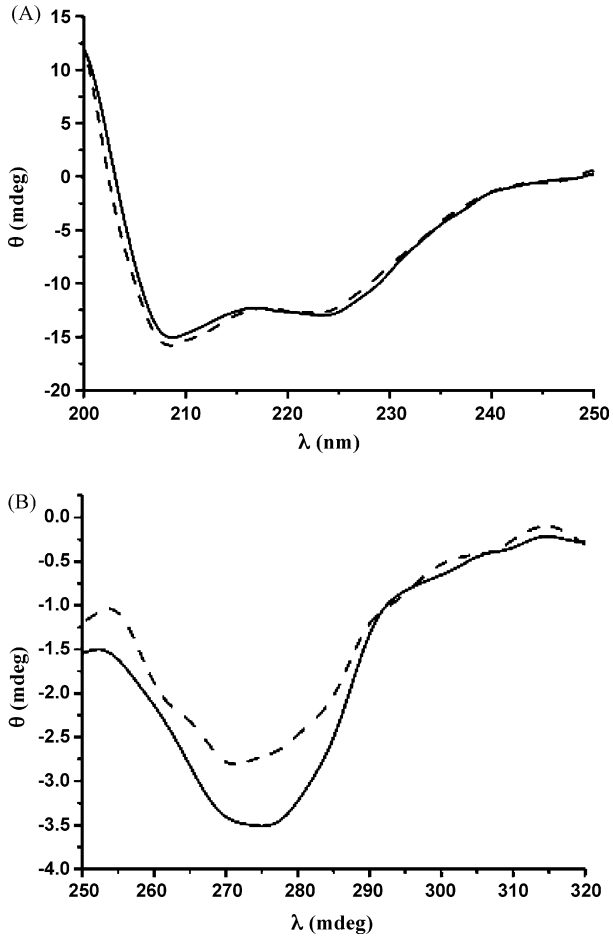

Fig. 3. (A) Far and (B) near CD spectra of (–) insulin and (- -) released insulin at a concentration of 150 μg/ml.

and release was evaluated in terms of its conformational change using CD spectroscopy, which had been widely applied to examining the conformation and self-association of insulin (Mercola et al., 1967; Goldman and Carpenter, 1974). In the CD spectrum of insulin, three negative CD-bands were usually observed at 208, 223 and 273 nm, which corresponded to α-helix, β-sheet and aromatic side-chains, respectively (Hind et al., 2000). The ratio of $\theta_{208}/\theta_{223}$ was used to provide a qualitative measure of insulin association (Pocker and Biswas, 1980), because an antiparallel β-structure was formed when two monomers dimerized, resulting in an increase of θ_{223} without an increase of θ_{208}. The near-ultraviolet CD-band at 273 nm primarily resulted from restriction of rotation of the aromatic side-chains, TyrB16, TyrB26, PheB24, and PheB25, between two insulin monomers in the dimer and between PheB1, PheB16, and TyrA14 in the insulin hexamer (Derwenda et al., 1989; Mark and Jeffrey, 1990). Therefore, attenuation of the 273 nm CD-band has been associated normally with conditions that reduce the aggregation of the molecule, such as dilution, alkaline pH and deprivation of zinc ions.

As shown in Fig. 3, released insulin exhibited a decreased θ_{223} while an increased θ_{208} compared to insulin solution in PBS at a concentration of 150 μg/ml. The $\theta_{208}/\theta_{223}$ ratio of released insulin was 1.23, which was slightly higher than that of insulin (1.15). Besides, θ_{273} of released insulin (−2.78) was attenuated as compared to that of insulin (−3.49). Such spectral features indicated that the overall conformation (tertiary structure) of insulin was not altered after drug loading and release, and the self-association tendencies of insulin were further restricted.

3.2.2. Bioactivity stability

The blood glucose level of mice following subcutaneous administration of 0.5 IU/kg of released insulin was 22.1 ± 3.7% of the initial level. No significant difference ($p > 0.05$) was observed as compared to the control, where 23.4 ± 3.6% of the initial blood glucose level was obtained. Therefore, it was concluded that bioactivity of insulin was well preserved after drug loading and release, which might be due to the conformational stability of insulin as mentioned in Section 3.2.1.

3.3. Trypsin and α-chymotrypsin inhibition

The capabilities of trypsin and α-chymotrypsin inactivation of the SPH-IPNs are shown in Figs. 4 and 5, respectively. In the case of the negative control, there was no degradation of insulin within 2 h. For the positive control, insulin was almost completely degraded and an increase in the enzyme concentration led to a faster degradation rate. In the presence of the SPH-IPNs, a significantly decrease in the degradation of insulin was observed, indicating that the polymers were able to partly inhibit the activity of two enzymes. When the concentration of trypsin and α-chymotrypsin solution was 6 and 8 μg/ml, respectively, SPH-IPN$_{192}$ and SPH-IPN$_{48}$ could effectively inhibit the enzyme activity, leaving over 90% of the insulin. As the enzyme concentration further increased, SPH-IPN$_{192}$ appeared to be more potent than SPH-IPN$_{48}$. For proteolytic enzyme inhibition of multifunctional polymers, there were several mechanisms including Ca^{2+} and Zn^{2+} deprivation (Lueβen et al., 1995), enzyme–polymer interaction that reduced free enzyme concentration and in part denatured the enzyme (Walker et al., 1999), and a reduction of pH below the optimum pH values of the pancreatic enzymes (Bai et al., 1996). In present investigation, the notable enzymatic inhibition of the SPH-IPNs might be attributed to their fast swelling abilities and binding properties of poly(acrylic acid-*co*-acrylamide) as well as *O*-CMC for Ca^{2+}. Fast swelling allowed the polymer to quickly entrap the enzyme solution (Dorkoosh et al., 2001) while chelating as well as adsorption properties of carboxyl groups on poly(acrylic acid-*co*-acrylamide) and *O*-CMC for Ca^{2+} led to the deprivation of Ca^{2+} from the structure of trypsin and α-chymotrypsin, which correspondingly inactivated these two enzymes (Lueβen et al., 1996). An improved enzyme inhibition of the SPH-IPNs with a higher *O*-CMC/monomer ratio might be due to the stronger affinity between Ca^{2+} and *O*-CMC, which bore many reactive functional groups for Ca^{2+} adsorption, apart from the –COOH group (Liang et al., 2004).

3.4. Ca^{2+} and Zn^{2+} binding

The Ca^{2+} and Zn^{2+} binding capacities of SPH-IPN$_{48}$ and SPH-IPN$_{192}$ are shown in Table 1. The majority of Ca^{2+} and

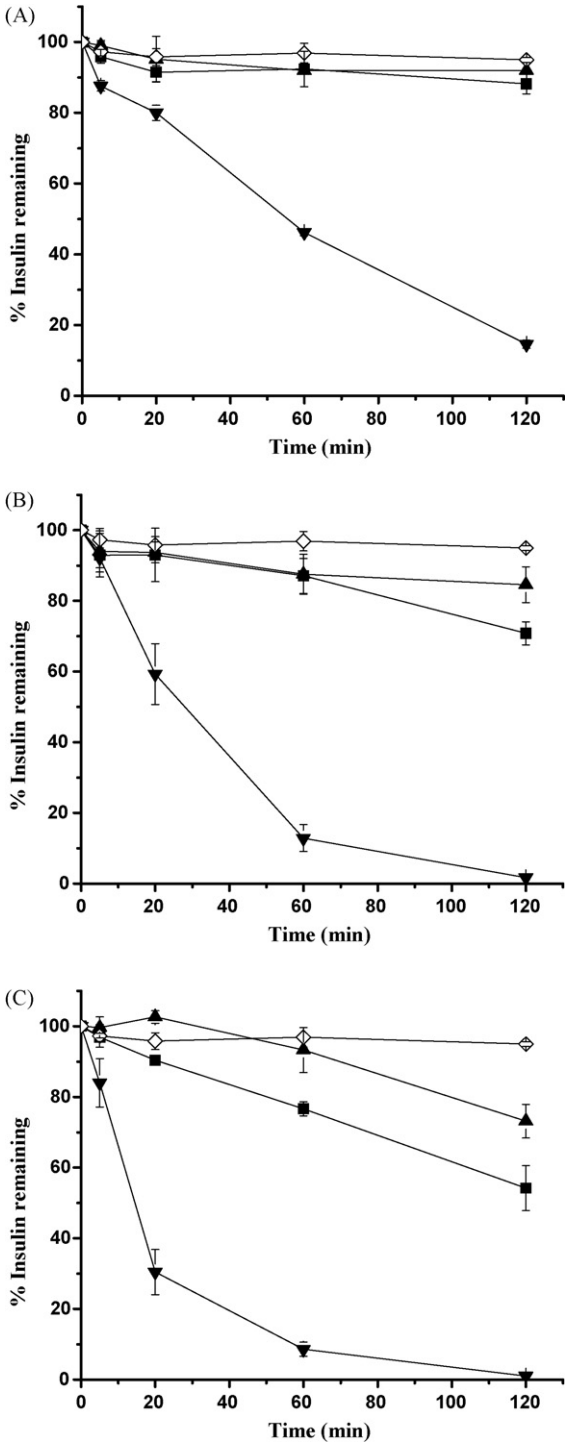

Fig. 4. Trypsin inhibition studies on SPH-IPNs with trypsin concentration of (A) 6 μg/ml, (B) 12 μg/ml, (C) 24 μg/ml, respectively. Each curve indicated: (■) SPH-IPN$_{48}$; (▲) SPH-IPN$_{192}$; (▼) positive control (insulin with trypsin solution); (◊) negative control (insulin solution). Data were expressed as mean ± S.D. of three experiments.

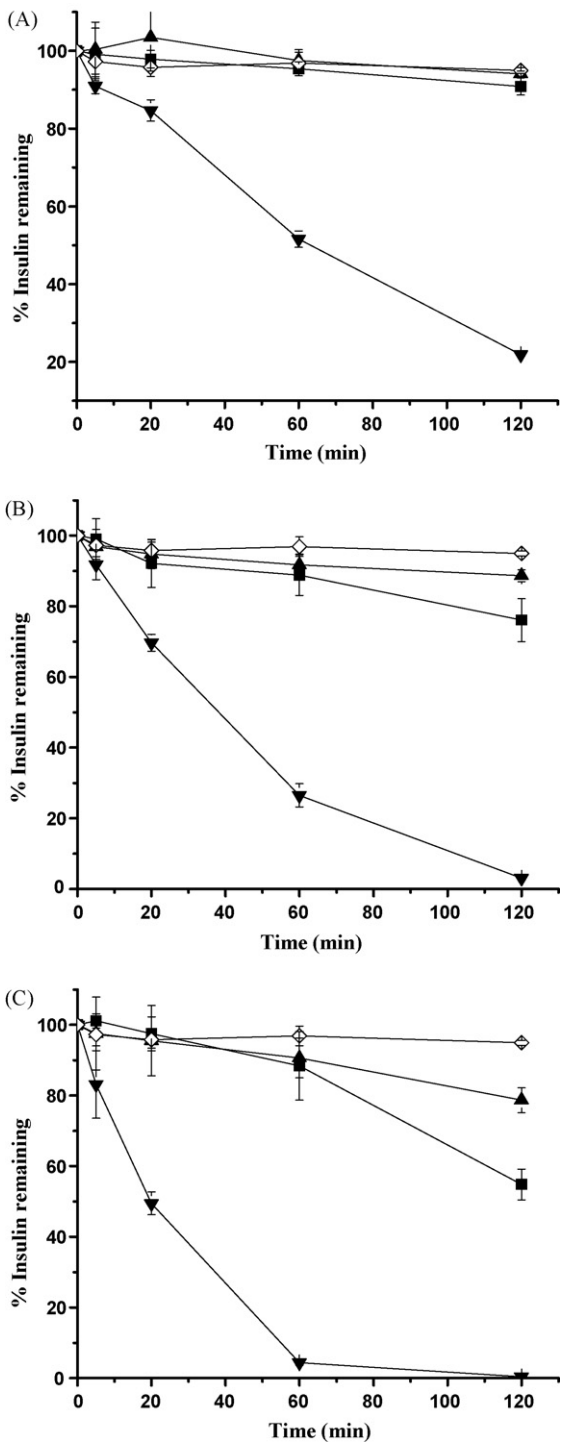

Fig. 5. α-Chymotrypsin inhibition studies on SPH-IPNs with α-chymotrypsin concentration of (A) 8 μg/ml, (B) 16 μg/ml, (C) 32 μg/ml, respectively. Each curve indicated: (■)SPH-IPN$_{48}$; (▲) SPH-IPN$_{192}$; (▼) positive control (insulin with α-chymotrypsin solution); (◊) negative control (insulin solution). Data were expressed as mean ± S.D. of three experiments.

Zn^{2+} (above 90%) were entrapped in the interconnected porous structure of the SPH-IPNs. Compared with SPH and SPHC reported by Dorkoosh et al. (2001), the SPH-IPNs possessed significantly improved Ca^{2+} binding capacity. Besides, SPH-IPN$_{192}$ exhibited higher binding capacity for Ca^{2+} and Zn^{2+} than SPH-IPN$_{48}$. Such result may be attributed to the stronger affinity between *O*-CMC and divalent metal ions (Liang et al., 2004; Sun and Wang, 2006a,b; Sun et al., 2006), apart from the binding capacity of poly(acrylates) for divalent metal cations (Kriwet and Kissel, 1996; Lueβen et al., 1996; Ameye et al.,

Table 1
M^{2+} binding studies (Ca^{2+} and Zn^{2+}) using SPH-IPN$_{48}$ and SPH-IPN$_{192}$

	Ca^{2+}		Zn^{2+}	
	SPH-IPN$_{48}$	SPH-IPN$_{192}$	SPH-IPN$_{48}$	SPH-IPN$_{192}$
FreeM^{2+} (%)[a]	9.09 ± 0.10	11.02 ± 4.76	0.46 ± 0.07	0.87 ± 0.10
Unbound M^{2+} (%)[a]	24.02 ± 2.82	8.62 ± 3.05	3.73 ± 0.17	1.68 ± 0.36
Bound M^{2+} (%)[a]	66.90 ± 2.88	80.36 ± 3.06	95.82 ± 0.11	97.5 ± 0.35
Binding capacity (mg)[b]	1.29 ± 0.06	1.55 ± 0.06	9.16 ± 0.01	9.32 ± 0.03

[a] Data were presented as % of total amount of M^{2+} added and expressed as mean ± S.D. of four experiments.
[b] Data were presented as the amount of bound M^{2+} per gram of the polymer.

2001). *O*-CMC bore many reactive functional groups, including carboxymethyl group, amino group, as well as both primary and secondary hydroxyl groups at the C-3, C-6 positions, respectively. These functional groups having interaction or synergistic action in the adsorption process provided adsorption sites for the divalent metal cation substrate, such as Ca^{2+} (Liang et al., 2004), Zn^{2+} (Sun and Wang, 2006b), Cu^{2+} (Sun and Wang, 2006a), and Pb^{2+} (Sun et al., 2006). In addition, cross-linked *O*-CMC revealed greater binding capacity for bivalent cations than *O*-CMC, as a result of the formation of three-dimensional structure that was favorable for capturing metal ions (Sun et al., 2006). The relatively higher amount of free Ca^{2+} for SPH-IPN$_{192}$ might be ascribed to its smaller swelling ratio as compared to SPH-IPN$_{48}$. The enhanced Ca^{2+} binding capacity of SPH-IPNs with higher *O*-CMC/monomer ratio also accounted for an improved enzymatic inhibition ability of the polymer as described in Section 3.3.

3.5. Mechanical fixation

After a horizontal force of around 4.38×10^{-4} N had been applied for 5 min, no movement of the SPH-IPNs was observed along the rat intestine segment. In contrast, the 0.5% Carbopol® 934 gel, which was a well-known muco-adhesive excipient, moved along the whole length of the intestine to the other end. Such results indicated that through mechanical fixation of the fully swollen SPH-IPNs to the intestinal wall, retentive property of the polymer was significantly improved.

3.6. In situ muco-adhesion

As shown in Fig. 6, more than 60% of the SPH-IPN$_{48}$ and SPH-IPN$_{192}$ were tightly adhered to the intestinal mucosa, which was significantly higher than Carbopol® 934. Fast swelling and large swelling ratios of the SPH-IPNs allowed them to rapidly adhere to the intestinal wall through mechanical pressure, thus leading to the improved muco-adhesive capacity of the polymer. The polyampholytic structure of *O*-CMC, which exerted an additional effect on mucosa adhesion due to formation of transitional physical cross-links between cationic and anionic groups carried by network chains (Zhao et al., 2001), also contributed to the enhanced muco-adhesion of the SPH-IPNs. In this manner, SPH-IPN$_{192}$ exhibited higher muco-adhesive capacity than SPH-IPN$_{48}$, which was in accordance with the in vitro muco-adhesion investigation (Yin et al., 2007).

3.7. Insulin transport ex vivo

The cumulative transport of insulin across rat intestine and colon is shown in Fig. 7, and the apparent permeability coefficient (P_{app}) values are depicted in Table 2. After application of SPH-IPN$_{192}$, the transport of insulin across the duodenum, jejunum, ileum and colon mucosa was enhanced two- to three-fold as compared to the controls. The potential of SPH-IPNs for the transport enhancement of insulin could be attributed to the combination of muco-adhesion and opening of the tight junctions. The muco-adhesive properties of SPH-IPNs provided a higher insulin concentration at the site of adhesion–absorption through intimate contact of the polymer with the mucus layer,

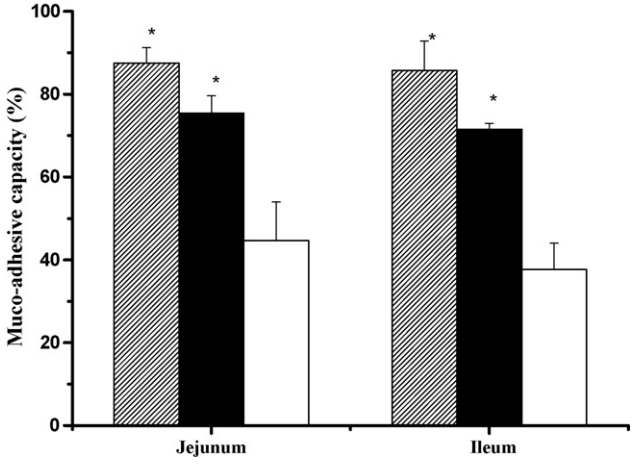

Fig. 6. In situ muco-adhesive capacities of (■) SPH-IPN$_{48}$, (▨) SPH-IPN$_{192}$, and (□) Carbopol® 934 in rat jejunum and ileum. Data were expressed as mean ± S.D. of three experiments. Statistically significant difference from Carbopol® 934: $^{*}p < 0.05$.

Table 2
Apparent permeability coefficients (P_{app}) for insulin across ex vivo isolated rat intestine and colon

Tissue	$P_{app} \times 10^{-7}$ (cm/s)[a]	
	Control	SPH-IPN
Duodenum	1.08 ± 0.19	3.77 ± 0.52*
Jejunum	5.49 ± 0.55	19.27 ± 3.19*
Ileum	5.99 ± 0.17	21.73 ± 3.37*
Colon	3.84 ± 0.24	12.84 ± 2.68*

[a] Data were expressed as mean ± S.D. of four experiments.
* Statistically significant difference from the control: $p < 0.05$.

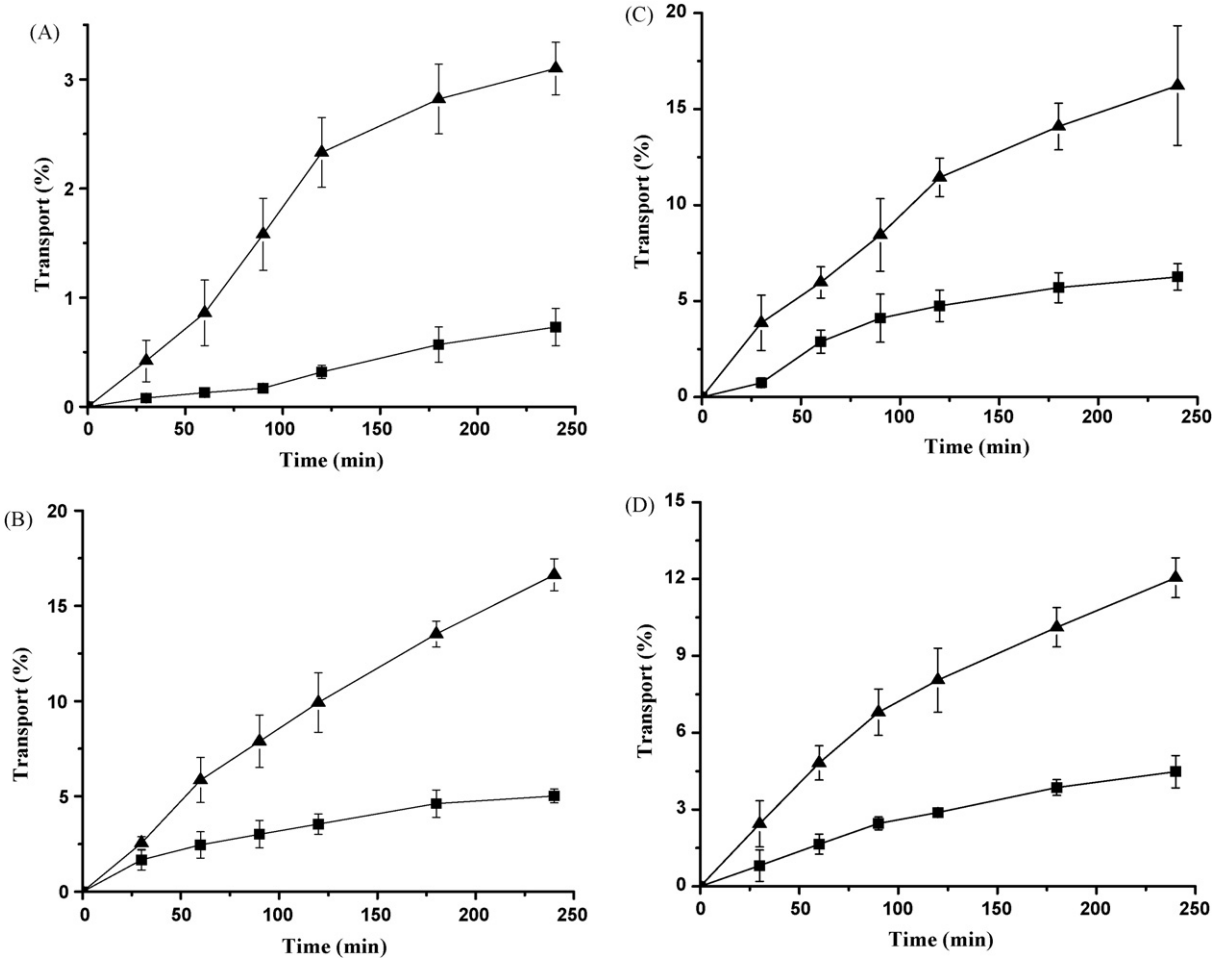

Fig. 7. Transport of insulin across rat (A) duodenum; (B) jejunum; (C) ileum; (D) colon ex vivo. Data were expressed as mean ± S.D. of three to five experiments and each curve indicated: (■) SPH-IPN$_{192}$; (▲) negative control.

which created a driving force for the paracellular passive transport (Hejazi and Amiji, 2003). After application of the SPH-IPNs, mechanical pressure upon the epithelia, water sorption of the polymer, and deprivation of endogenous Ca^{2+} were responsible for the opening of the tight junctions. The mechanical pressure of the swollen polymer upon the gut wall would embrace the columnar epithelial cells and make a gap between the cells where the tight junctions were located, thereby causing the opening of these junctions (Dorkoosh et al., 2002a). Large water absorption of the SPH-IPNs would result in cell dehydration and subsequent cell shrinking, which ultimately led to the expansion of the spaces between the cells (Haas and Lehr, 2002). On the other hand, in order to compensate such water loss and maintain the homeostasis of the intestinal cells, tight junctions were opened to facilitate fast uptake of water molecules (Dorkoosh et al., 2002a). With the ability of the SPH-IPNs to bind Ca^{2+} as observed in Section 3.4, free extracellular Ca^{2+} that were essential for the cells to maintain intercellular contacts could be removed. This induced the modification of the cell physiology such as disruption of actin filaments and adherens junctions, diminished cell adhesion and activation of protein kinases, thus favoring the opening of the tight junctions (Citi, 1992).

3.8. Hypoglycaemic effect following oral administration of insulin-loaded SPH-IPNs

Fig. 8 shows the plasma glucose level–time profiles following subcutaneous injection of insulin solution and oral administration of insulin solution, blank SPH-IPN$_{144}$, and insulin-loaded SPH-IPN$_{144}$ to healthy rats. No hypoglycaemic effect was observed during administration of insulin solution (40 IU/kg), confirming the well-known inefficiency of insulin absorption via the oral route in the absence of an appropriate carrier. After oral administration of insulin-loaded SPH-IPNs (40 IU/kg), the blood glucose level remarkably decreased at 2 h, achieving a maximum hypoglycaemic effect at 4 h (60% of the initial level) and continuing up to 6 h. For the negative control where blank SPH-IPNs were administered, the plasma glucose level maintained close to the baseline over the course of the study period. Such results demonstrated that the SPH-IPN itself had no hypoglycaemic effect while significantly enhanced the absorption of insulin from rat intestine. The $[AAC]_{p.o.}$ and $[AAC]_{s.c.}$ for 0–8 h were 12987 ± 1727 and 7882 ± 2291, respectively, indicating a relative pharmacological availability (PA) of 4.1 ± 0.5%.

The efficacy of the SPH-IPNs as a peroral carrier for insulin was attributed to their capacities of enzymatic inhibition, perme-

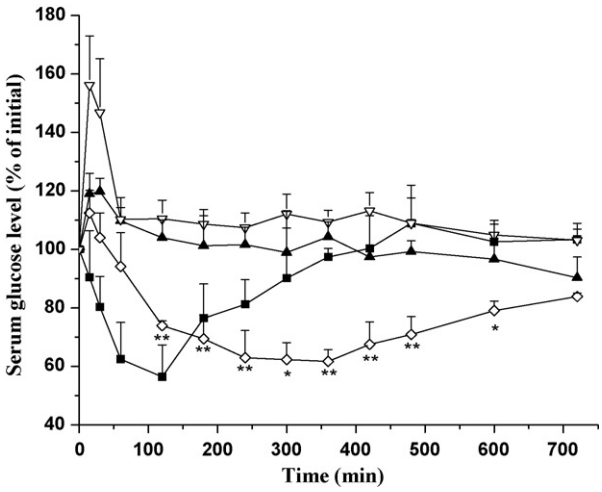

Fig. 8. Serum glucose level versus time profiles following administration of various formulations: (■) subcutaneous injection (1 U/kg); (◊) oral administration of insulin-loaded SPH-IPN$_{144}$ (40 U/kg); (▲) oral administration of blank SPH-IPN$_{144}$; (▽) oral administration of insulin solution. Each point represented mean ± S.D. of four experiments. Statistically significant difference from blank SPH-IPNs: $^{*}p < 0.05$, $^{**}p < 0.01$.

ation enhancement and muco-adhesion. Insulin incorporated in the SPH-IPNs could be effectively protected from the enzymes in the intestine, which led to improved absorption of insulin. As a result of opening of tight junctions of the SPH-IPNs, the insulin absorption through the intestinal epithelium was enhanced. Both the muco-adhesion and the mechanical attachment of the swollen SPH-IPNs would lead to a prolonged retention time in the intestine, favoring a site-specific drug targeting and an improved drug absorption.

4. Conclusions

Insulin release was restricted in acidic medium while rapid and complete release occurred in neutral conditions. At ionic strength of 0.1 M, insulin release was rapid and complete. Conformation as well as bioactivity of insulin was maintained following drug loading and release, which was favorable for drug absorption and pharmaceutical activity. Insulin-loaded SPH-IPNs showed a significant hypoglycemic effect when orally administered, which might be attributed to the desired properties of the SPH-IPNs, including trypsin and α-chymotrypsin inhibition based on their Ca^{2+} binding abilities and enzyme entrapment, muco-adhesion from mechanical attachment and the polyampholytic structure of *O*-CMC, and absorption enhancement related to the opening of the tight junctions on the epithelium membrane. In conclusion, the SPH-IPN should be a desirable delivery vehicle for absorption of insulin and other peptide drugs via the oral route.

Acknowledgement

The authors are thankful for the financial support from Science and Technology Commission of Shanghai Municipality of China (No. 054319934).

References

Aboubakar, M., Couvreur, P., Pinto-Alphandary, H., Gouritin, B., Lacour, B., Farinotti, R., Puisieux, F., Vauthier, C., 2000. Insulin-loaded nanocapsules for oral administration: in vitro and in vivo investigation. Drug Dev. Res. 49, 109–117.

Ameye, D., Voorspoels, J., Foreman, P., Tsai, J., Richardson, P., Geresh, S., Remon, J.P., 2001. Trypsin inhibition, calcium and zinc ion binding of starch-*g*-poly(acrylic acid) copolymers and starch/poly(acrylic acid) mixtures for peroral peptide drug delivery. J. Control. Release 75, 357–364.

Aoki, Y., Morishita, M., Asai, K., Akikusa, B., Hosoda, S., Takayama, K., 2005. Regional dependent role of the mucous/glycocalyx layers in insulin permeation across rat small intestinal membrane. Pharm. Res. 22, 1854–1862.

Asada, H., Douen, T., Waki, M., Adachi, S., Fujita, T., Yamamoto, A., Muranishi, S., 1995. Absorption characteristics of chemically modified-insulin derivatives with various fatty acids in the small and large intestine. J. Pharm. Sci. 84, 682–687.

Bai, J.P.F., Chang, L.L., Guo, J.H., 1996. Effects of polyacrylic polymers on the degradation of insulin and peptide drugs by chymotrypsin and trypsin. J. Pharm. Pharmacol. 48, 17–21.

Chinese Pharmacopoeia, vol. 2, 2000. Chinese Pharmacopeial Convention, China, pp. 439.

Citi, S., 1992. Protein kinase inhibitors prevent junction dissociation by low extracellular calcium in MDCK epithelial cells. J. Cell Biol. 117, 169–178.

Derwenda, U., Derwenda, Z., Dodson, G.G., Hubbard, R.E., Korber, F., 1989. Molecular structure of insulin: the insulin monomer and its assembly. Br. Med. Bull. 45, 4–18.

Dorkoosh, F.A., Borchard, G., Rafiee-Tehrani, M., Verhoef, J.C., Junginger, H.E., 2002a. Evaluation of superporous hydrogel (SPH) and SPH composites in porcine intestine ex vivo: assessment of drug transport, morphology effect, and mechanical fixation to intestinal wall. Eur. J. Pharm. Biopharm. 53, 161–166.

Dorkoosh, F.A., Verhoef, J.C., Borchard, G., Rafiee-Tehrani, M., Junginger, H.E., 2001. Development and characterization of a novel peroral peptide drug delivery system. J. Control. Release 71, 307–318.

Dorkoosh, F.A., Setyaningsih, D., Borchard, G., Rafiee-Tehrani, M., Verhoef, J.C., Junginger, H.E., 2002b. Effects of superporous hydrogels on paracellular drug permeability and cytotoxicity studies in Caco-2 cell monolayers. Int. J. Pharm. 241, 35–45.

Dorkoosh, F.A., Verhoef, J.C., Ambagts, M.H.C., Rafiee-Tehrani, M., Borchard, G., Junginger, H.E., 2002c. Peroral delivery system based on superporous hydrogel polymers: release characteristics of the peptide drugs buserelin, octreotide and insulin. Eur. J. Pharm. Sci. 15, 433–439.

Goldman, J., Carpenter, F.H., 1974. Zinc binding, circular dichroism, and equilibrium sedimentation studies in insulin (bovine) and several of its derivatives. Biochemistry 13, 4566–4574.

Haas, J., Lehr, C.M., 2002. Developments in the area of bioadhesive drug delivery systems. Expert Opin. Biol. Ther. 2, 287–298.

Hejazi, R., Amiji, M., 2003. Chitosan-based gastrointestinal delivery systems. J. Control. Release 89, 151–165.

Hind, K., Koh, J.J., Joss, L., Liu, F., Baudys, M., Kim, S.W., 2000. Synthesis and characterization of poly(ethylene glycol)-insulin conjugates. Bioconjug. Chem. 11, 195–201.

Kriwet, B., Kissel, T., 1996. Interactions between bioadhesive poly(acrylic acid) and calcium ions. Int. J. Pharm. 127, 135–145.

Liang, P., Zhao, Y., Shen, Q., Wang, D., Xu, D., 2004. The effect of carboxymethyl chitosan on the precipitation of calcium carbonate. J. Cryst. Growth 261, 571–576.

Lueβen, H.L., Borchard, G., Verhoef, J.C., Lehr, C.-M., Boer, A.G., Junginger, H.E., 1995. Mucoadhesive polymers in peroral peptide drug delivery. II. Carbomer and polycarbophil are potent inhibitors of the intestinal proteolytic enzyme trypsin. Pharm. Res. 12, 1293–1298.

Lueβen, H.L., Bohner, V., Perard, D., Langguth, P., Verhoef, J.C., Boer, A.G., Merkle, H.P., Junginger, H.E., 1996. Mucoadhesive polymers in peroral peptide drug delivery. V. Effect of poly(acrylates) on the enzymatic degradation of peptide drugs by intestinal brush border membrane vesicles. Int. J. Pharm. 141, 39–52.

Mark, A.E., Jeffrey, P.D., 1990. The self-association of zinc-free bovine insulin—4 model patterns and their significance. Biol. Chem. Hoppe-Seyler 371, 1165–1174.

Marschutz, M.K., Caliceti, P., Bernkop-Schnurch, A., 2000. Design and in vivo evaluation of an oral delivery system for insulin. Pharm. Res. 17, 1468–1474.

Mercola, D.A., Morris, J.W.S., Arquilla, E.R., Bromer, W.W., 1967. The ultraviolet circular dichroism of bovine insulin and desoctapeptide insulin. Biochim. Biophys. Acta 133, 224–232.

Mesiha, M., Plakogiannis, F., Vejosoth, S., 1994. Enhanced oral absorption of insulin from desolvated fatty acid-sodium glycocholate emulsions. Int. J. Pharm. 111, 213–216.

Morishita, M., Aoki, Y., Sakagami, M., Nagai, T., Takayama, K., 2004. In situ ileal absorption of insulin in rats: effects of hyaluronidase pretreatment diminishing the mucous/glycocalyx layers. Pharm. Res. 21, 309–316.

Pocker, Y., Biswas, S.B., 1980. Conformational dynamics of insulin in solution. Circular dichroic studies. Biochemistry 19, 5043–5049.

Polnok, A., Verhoef, J.C., Borchard, G., Sarisuta, N., Junginger, H.E., 2004. In vitro evaluation of intestinal absorption of desmopressin using drug-delivery systems based on superporous hydrogels. Int. J. Pharm. 269, 303–310.

Radwant, M.A., Aboul-Enein, H.Y., 2002. The effect of oral absorption enhancers on the in vivo performance of insulin-loaded poly(ethylcyanoacrylate) nanospheres in diabetic rats. J. Microencapsul. 19, 225–235.

Saffran, M., Pansky, B., Budd, G.C., Williams, F.E., 1997. Insulin and the gastrointestinal tract. J. Control. Release 46, 89–98.

Sun, S., Wang, A., 2006a. Adsorption kinetics of Cu(II) ions using *N*,*O*-carboxymethyl-chitosan. J. Hazard. Mater. B 131, 103–111.

Sun, S., Wang, A., 2006b. Adsorption properties and mechanism of cross-linked carboxymethyl-chitosan resin with Zn(II) as template ion. React. Func. Polym. 66, 819–826.

Sun, S., Wang, L., Wang, A., 2006. Adsorption properties of crosslinked carboxymethyl-chitosan resin with Pb(II) as template ions. J. Hazard. Mater. 136, 930–937.

Takeuchi, H., Yamamoto, H., Niwa, T., Hino, T., Kawashima, Y., 1996. Enteral absorption of insulin in rats from mucoadhesive chitosan-coated liposomes. Pharm. Res. 13, 896–901.

Walker, G.F., Ledger, R., Tucker, I.G., 1999. Carbomer inhibits tryptic proteolysis of luteinizing hormone-releasing hormone and *N*-a-benzoyl-L-arginine ethyl ester by binding the enzyme. Pharm. Res. 16, 1074–1080.

Yin, L., Fei, L., Cui, F., Tang, C., Yin, C., 2007. Superporous hydrogels containing poly(acrylic acid-*co*-acrylamide)/*O*-carboxymethyl chitosan interpenetrating polymer networks. Biomaterials 28, 1258–1266.

Zhao, X., Kato, K., Fukumoto, Y., Nakamae, K., 2001. Synthesis of bioadhesive hydrogels from chitin derivatives. Int. J. Adhes. Adhes. 21, 227–232.

Ziv, E., Kidron, M., Raz, I., Krausz, M., Blatt, Y., Rotman, A., Bar-On, H., 1994. Oral administration of insulin in solid form to nondiabetic and diabetic dogs. J. Pharm. Sci. 83, 792–794.